

# Performance limits of direct cryogenically cooled silicon monochromators

Wah-Keat Lee, Patricia Fernandez, and Denny M. Mills

User Program Division, Advanced Photon Source, Argonne National Laboratory, Argonne, IL 60439 USA

## Introduction

Taking advantage of the opportunity to have two undulators in series on the 1-ID beamline, we have been able to map out quantitatively the thermal performance limits of the direct cryogenically cooled silicon monochromator. While finite element analysis methods can be used to calculate the performance, the calculations in this case can be quite tricky and complicated due to the nonlinear and temperature-dependent nature of the thermal properties of silicon at cryogenic temperatures. Our results show that if we limit the size of the white beam to the undulator central cone FWHM, the current cryogenically cooled silicon monochromator will perform well ( $< 2$  arc seconds thermal distortion) at up to twice the normal 100 mA, single undulator thermal loads [1].

## Methods and Materials

The schematic and dimensions of the cryogenically cooled silicon monochromator are shown in Figure 1.

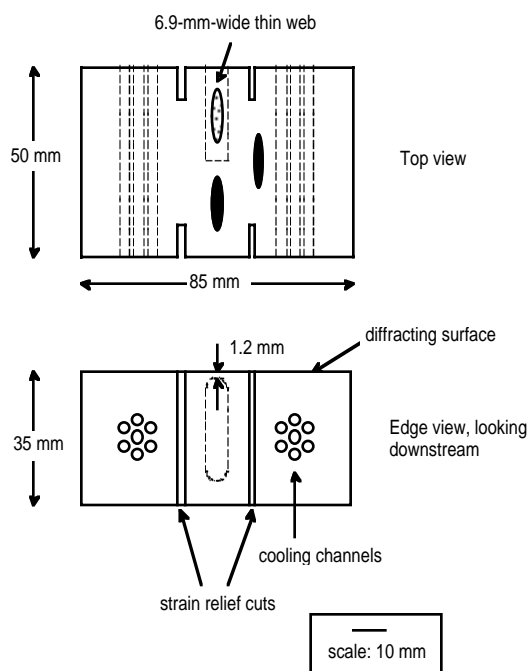


Figure 1: Schematic of the cryogenically cooled silicon monochromator. The diffraction planes are (111).

We monitor the performance of the monochromator by measuring the FWHM of double-crystal rocking-curve widths at the higher-order  $(333)\text{-}\lambda/3$  reflections. The experimental setup is shown in Figure 2. Measurements were performed on both the thin web (dotted oval in Figure 1) and the thick parts (filled ovals in Figure 1) of the crystal on the crystal. The measured powers were lower than the XOP [2] calculations by about 10-20%.

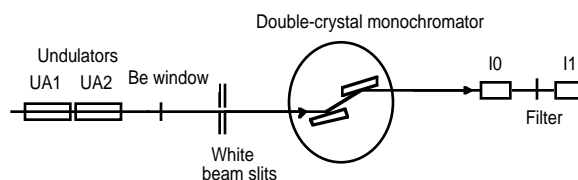


Figure 2: Schematic of experimental setup.

## Results

In the simplest approximation [3], in which the incident power is absorbed on the surface, the thermal slope error on the monochromator is proportional to  $Q$ , the surface absorbed power density and  $k/\alpha$ , where  $k$  is the thermal conductivity (W/cm) and  $\alpha$  is the thermal expansion coefficient (1/K). Since  $k/\alpha$  is dependent on temperature, the total absorbed power (which influences the average crystal temperature) should be one of the thermal parameters affecting the slope error. At third-generation synchrotron sources, the critical energy of the radiation can be quite high ( $\sim 10\text{-}30$  keV). Thus, power absorption length in the crystal can be in the millimeter range, while x-ray extinction lengths in this energy regime are in the micron range. Therefore, the assumption that all the incident power is absorbed on the surface is not valid. Instead, based on the extinction lengths, we choose to associate  $Q$  with the average absorbed power density in the first  $10\ \mu\text{m}$  of silicon.

Figure 3 summarizes the data for the thick part of the crystal. The hyperbolic curve is a guide to the eye: the data suggest that, if the heat variables fall to the left and below this curve, the crystal should have less than 2 arc seconds thermal distortion. The other lines on the plot are 'heat-load tuning curves' in the 7–20 keV range. These curves represent the thermal loads on the crystal under the assumption that the undulator is tuned such that the desired energy is the first or third undulator harmonic. In the 7–12 keV range, the first harmonic is usually used, while in the 12–20 keV range, the third harmonic is used.

To better illustrate the dramatic change in the rocking-curve width with the thermal load, Figure 4 is a three-dimensional surface plot of the same data.

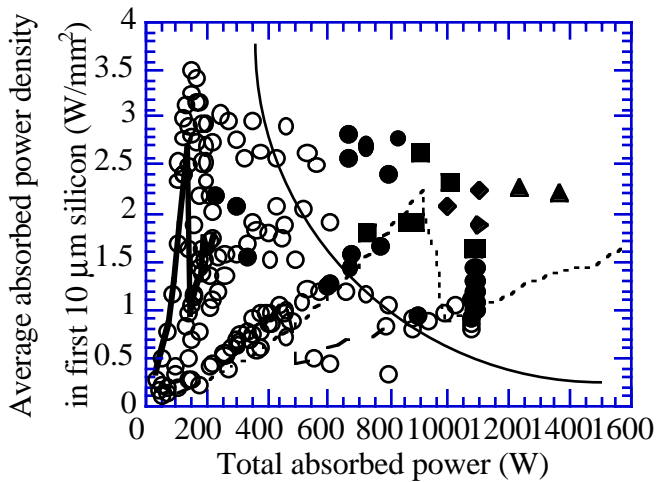


Figure 3: A plot of all the data collected on the *thick* part of the crystal. The symbols represent the following: open circles (O) -  $I1 \text{ FWHM} < 2''$ , filled circles (●) -  $2'' < I1 \text{ FWHM} < 10''$ , filled squares (■) -  $10'' < I1 \text{ FWHM} < 20''$ , filled diamonds (◆) -  $20'' < I1 \text{ FWHM} < 30''$  and filled triangles (▲) -  $I1 \text{ FWHM} > 30''$ . The hyperbolic-like curve is a guide to the eye: the data suggest that for heat load variables to the left and below this curve, the thermal distortions will be less than  $2''$ . Three “heat-load tuning curves” are also shown. Dashed line: 3 mm H x 2 mm V white beam single undulator, 100 mA ring current; dotted line: 3 mm H x 2 mm V white beam single undulator, 200 mA ring current;

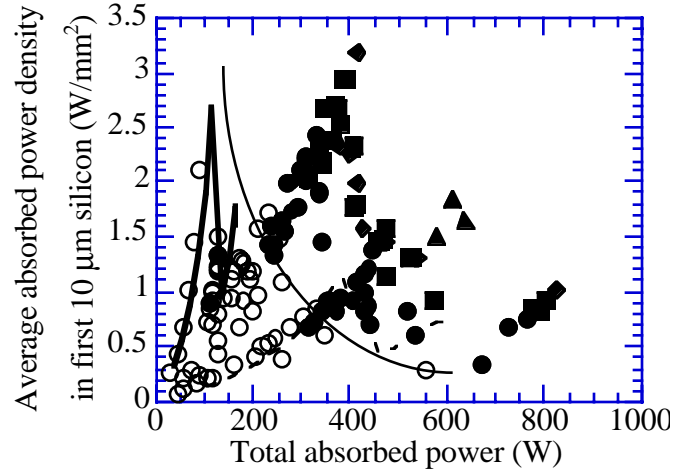


Figure 5: A plot of all the data collected on the *thin* part of the crystal. The symbols represent the following: open circles (O) -  $I1 \text{ FWHM} < 2''$ , filled circles (●) -  $2'' < I1 \text{ FWHM} < 10''$ , filled squares (■) -  $10'' < I1 \text{ FWHM} < 20''$ , filled diamonds (◆) -  $20'' < I1 \text{ FWHM} < 30''$  and filled triangles (▲) -  $I1 \text{ FWHM} > 30''$ . The hyperbolic-like curve is a guide to the eye: the data suggest that, for heat-load variables to the left and below this curve, the thermal distortions will be less than  $2''$ . Two “heat-load tuning curves” are also shown. Dashed line: 3 mm H x 2 mm V white beam single undulator, 100 mA ring current; thick solid line: 1.5 mm H x 0.5 mm V white beam single undulator, 200 mA ring current.

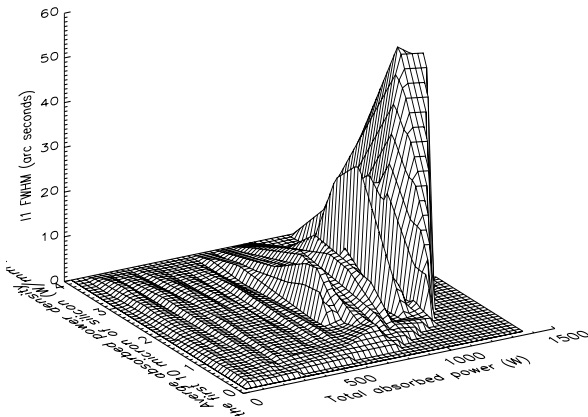


Figure 4: A three-dimensional rendition of the data from Figure 3.

## Discussion

These results clearly show that for the crystal shown in Figure 1, the thick part of the crystal performs much better than the thin part. Although the thick part absorbs more power, it has better thermal conduction paths for heat dissipation. The results also show that the actual power absorption profile as a function of depth in the crystal is an important consideration; especially at third-generation synchrotron sources where the critical energy is high. This can be seen from the data plots: at the same total absorbed power, the measured widths are larger for higher average absorbed power density in the first  $10 \mu\text{m}$  of silicon. Finally, the data show that this monochromator will perform well at thermal loads twice the current standard APS operation at 100 mA with a single undulator A.

## Acknowledgments

We wish to thank Felix Krasnicki and Josef Maj for their assistance in fabrication and characterization of the crystals and the SRI-CAT sector 1 staff for their assistance on the beamline. Use of the Advanced Photon Source was supported by the U.S. Department of Energy, Basic Energy Sciences, Office of Science, under Contract No. W-31-109-Eng-38. single undulator A.

## References

- [1] W.-K. Lee, P. Fernandez, and D.M. Mills, *J. Synchrotron Rad.* **7**, 12–17 (2000).
- [2] R.J. Dejus and M.S. del Rio, *Rev. Sci. Instrum.* **67(9)** CDROM (1996).
- [3] V.I. Subbotin, V.S. Kolesov, Y.A. Kuzmin, and V.V. Kharitonov, *Sov. Phys. Dokl.* **33(8)**, 633–635 (1998).